Identifying the "true" repeat unit of a copolymer using time-resolved electron paramagnetic resonance spectroscopy: a case study involving PNDIT2, NDI-T2 and T-NDI-T

Clemens Matt,[†,‖] Rukiya Matsidik,[‡,¶] Deborah L. Meyer,[†] Mirjam Schröder,[§] Michael Sommer,[¶] and Till Biskup*[,†,‖]

†*Institut für Physikalische Chemie, Albert-Ludwigs-Universität Freiburg, Albertstraße 21, 79104 Freiburg, Germany*
‡*Institut für Makromolekulare Chemie, Albert-Ludwigs-Universität Freiburg, Stefan-Meier-Straße 31, 79104 Freiburg, Germany*
¶*Lehrstuhl Polymerchemie, Technische Universität Chemnitz, Straße der Nationen 62, 09111 Chemnitz, Germany*
§*Leibnitz-Institut für Katalyse e.V., Albert-Einstein-Straße 29a, 18059 Rostock, Germany*
‖*Current Address: Physikalische Chemie, Universität des Saarlandes, Campus B2 2, 66123 Saarbrücken, Germany*

E-mail: research@till-biskup.de

Abstract

Semiconducting polymers promise to revolutionise the way electronic devices can be built and deployed for a vast array of applications ranging from light-energy conversion to sensors to thermoelectric generators. Conjugated push-pull copolymers consisting of alternating donor and acceptor moieties are at the heart of these applications, due to the large tunability of their electronic structure. Hence, knowing the repeat unit and thus the chromophore of these materials is essential for a detailed understanding of the structure–function relationship of conjugated polymers used in organic electronics applications. Therefore, spectroscopic tools providing the necessary molecular resolution that allows to discriminate between different building blocks and to decide which one actually resembles the electronic structure of the polymer are of utmost importance. Time-resolved electron paramagnetic resonance (TREPR) spectroscopy is both, perfectly suited for this task and clearly superior to optical spectroscopy, particularly when supported by quantum-chemical calculations. This is due to its molecular resolution and unique capability of using light-induced triplet states to probe the electronic structure as well as the impact of the local environment. Here, we demonstrate the power of this approach for the polymer PNDIT2 (poly[*N*,*N*'-bis(2-octyldodecyl)-naphthalene-1,4,5,8-bis(dicarboximide)-2,6-diyl]-*alt*-5,5'-(2,2'-bithiophene)) revealing NDI-T2 unambiguously as the "true" repeat unit of the polymer, representing the chromophore. The alternative building block T-NDI-T has a markedly different electronic structure. These results are of high importance for the rational design of conjugated polymers for organic electronics applications.

Graphical TOC Entry

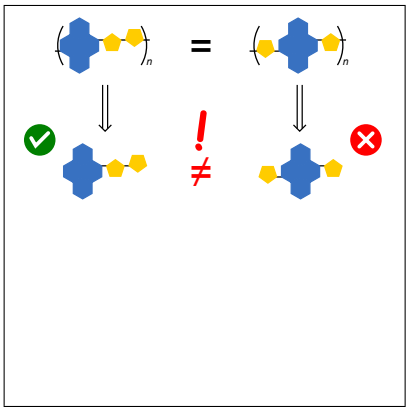

Keywords

conjugated push-pull copolymers, repeat unit, building block, electronic structure, triplet states, electron paramagnetic resonance

Introduction

Ever since the discovery of conducting polymers[1,2] that consecutively led to awarding the Nobel prize in chemistry to Alan J. Heeger, Alan G. MacDiarmid and Hideki Shirakawa in 2000 have these materials inspired the imagination of physicists, chemists, and engineers alike. (Semi-)conducting polymers not only allow to address fundamental questions of physics and chemistry of soft matter, but open the doors to an entirely new class of devices,[3] combining the power of tremendously miniaturised electronic circuits with the flexibility and ease of processing of polymeric materials. While in the first decades, mostly homopolymers have been investigated, more recently, push-pull copolymers consisting of alternating donor and acceptor moieties are increasingly important. They offer much better tunability of their electronic structure, i.e. their HOMO or LUMO level, ultimately leading to better efficiency compared to homopolymers for many applications.[4–6] However, this comes at the prize of a much more complicated electronic structure, and it is not necessarily obvious from the chemical structure which is the "true" repeat unit of such a polymer. Knowing the repeat unit is essential for characterising and understanding the electronic structure and hence the parameters determining efficiency of these materials.

While different repeat units result in the same polymer, for push-pull copolymers often a single repeat unit can serve as a model for the actual chromophore[7,8] dictating the electronic structure, as shown for PCDTBT[9,10] and PNDIT2[11]. Investigating representative repeat units instead of the entire polymer is relevant both for from a theoretical and experimental perspective. Quantum-chemical calculations depend non-linearly on the number of atoms, and the computing time dramatically increases by a factor of 10–50 between fragments consisting of n repeat units with $n = 1$ and $n = 3$, the latter serving as model for the polymer chain. Usually, calculations for $n = 1$ already take a few hours. In order to obtain reliable results from quantum-chemical calculations, functionals and basis sets for DFT and potentially even

methods need to be varied, sampling a large parameter space. Furthermore, advanced calculations are only feasible for small molecules.[12] From an experimental point of view, small molecules often exhibit better signal-to-noise ratio in spectroscopy compared to polymers. Furthermore, additional effects *e.g.* from morphology[13,14] and exciton mobility[13,15] can be excluded. Therefore, it is of utmost importance to unequivocally identify the repeat unit resembling the chromophore of the polymer and only use this for further detailed investigation. This requires a combined approach of spectroscopic methods with sufficient resolution to discriminate between different possible candidates, synthetic chemistry providing the different structures, and comparison with the polymer. Here we demonstrate the power of this approach for the polymer poly[*N*,*N*'-bis(2-octyldodecyl)-naphthalene-1,4,5,8-bis(dicarboximide)-2,6-diyl]-*alt*-5,5'-(2,2'-bithiophene) (PNDIT2) and two possible repeat units, namely T-NDI-T and NDI-T2 (cf. Fig. 1), using time-resolved EPR spectroscopy and quantum-chemical calculations. The clearly superior molecular resolution of TREPR spectroscopy compared to optical methods proves crucial and allows for unequivocally identifying the actual repeat unit.

PNDIT2 is a prominent example of naphthalenediimide (NDI) based polymers[16] predominantly used as acceptor materials[17,18] or n-type semiconductors[19] in organic electronics. It is renowned for its excellent electron mobility[11,14,20–24] and consists of alternating units of NDI and thiophenes (T) which themselves act as electron acceptors (A) and donors (D), respectively. The interaction of these units determines the electronic structure of the polymer, hence a detailed characterisation and understanding is of utmost importance for guiding the targeted design of new materials.

In case of the polymer PNDIT2, two potential repeat units are possible: T-NDI-T and NDI-T2 as presented in Fig. 1. While upon polymerisation both units result in the same polymer, the molecules as such are two distinct chromophores with tremendously different electronic structure. This immediately raises the question which one reflects the electronic

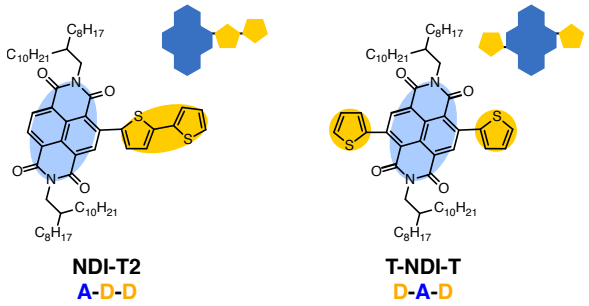

Figure 1: Chemical structures of NDI-T2 and T-NDI-T. The molecules each consist of one naphthalenediimide (NDI) and two thiophene units (T), respectively. Whereas the NDI moiety acts as an electron acceptor (A), the T units act as donors (D). The pictograms shown in the top right corner of each of the structures are used hereafter for simplicity.

structure of the polymer PNDIT2. Steady-state optical spectroscopy is of no help here, as it lacks the resolution necessary to reveal the details of the electronic structure. Therefore, time-resolved electron paramagnetic resonance (TREPR) spectroscopy[25–27] complemented by quantum-chemical calculations was employed on both small molecules and compared with the results previously obtained for the polymer[11] to address this question. Due to its molecular resolution, EPR spectroscopy is superior here to optical spectroscopy suffering from broad, overlapping and often unstructured lines. Light-induced short-lived triplet states probed by TREPR spectroscopy have been shown to be particularly sensitive to the local molecular environment, both in terms of morphology[13,14,28] and electronic structure[10,11,15,29]. Therefore, TREPR spectroscopy in conjunction with quantum-chemical calculations is the method of choice for analysing the electronic structure of both potential repeat units of PNDIT2 with molecular resolution, and for answering the question which of them is the actual repeat unit of the polymer.

Results

For a first overview, steady-state absorption spectra in the UV/visible region were recor-

ded for both potential repeat units of PNDIT2 (cf. Fig. 2). Both show an absorption band in the visible region which can be ascribed to a charge-transfer (CT) band[11]. The CT band of NDI-T2 is red-shifted and broader compared to that of T-NDI-T, hinting at a larger delocalisation of the singlet exciton in the former molecule. The absorption bands in the near-UV with the two characteristic features at 357 and 377 nm are associated to a π–π* transition of the NDI moiety[30] and more pronounced in case of T-NDI-T. As in other studies of push–pull copolymers[9–11], the intensity of the π–π* transition is larger than that of the CT band. This effect is more prominent for NDI-T2. Absorption spectra of the polymer are qualitatively identical, with a broad CT band in the visible wavelength range, red-shifted as expected compared to both potential building blocks, and a sharp π–π* transition in the near UV region[11]. Simply comparing the spectra shown in Fig. 2 with the one of the polymer does not allow to conclude which molecule is the true repeat unit of PNDIT2 in terms of the electronic structure of its chromophore, and the differences in delocalisation provide no hint in this regard, as T-NDI-T and NDI-T2 are identical in length. Therefore, we used TREPR spectroscopy known for its high molecular resolution to investigate the light-induced, short-lived triplet states of both molecules and compared the result with those obtained previously for the polymer[11,14].

TREPR spectroscopy is one of the few methods that allows to directly probe light-induced short-lived triplet states. While the time-dependent EPR signal intensity is recorded for subsequent magnetic field positions, often only slices along the magnetic field axis are investigated, as they allow to extract the relevant parameters. Furthermore, triplet state kinetics cannot readily be extracted from the TREPR time profiles.[31]

TREPR spectra of the light-induced triplet states of T-NDI-T and NDI-T2 are shown in Fig. 3, together with the spectrum obtained previously for the polymer[11,14]. The spectra have been extracted from the full two-dimensional dataset (time vs. magnetic field)

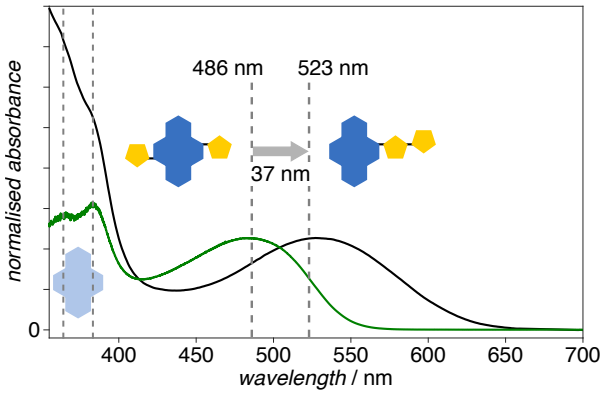

Figure 2: Absorption spectra of T-NDI-T and NDI-T2 in 1-CN. The prominent absorption band in the visible range of the spectrum centred at about 486 and 523 nm, respectively, is attributed to a charge-transfer (CT) between donor and acceptor moieties. The band in the near-UV region is attributed to a π–π* transition of the NDI moiety. For comparison, both spectra are normalised on the same CT band maximum. The vertical dotted lines in the visible range represent the excitation wavelengths used for TREPR spectroscopy (486 and 523 nm, cf. Fig. 3). Those at 357 and 377 nm mark the transitions attributed to the NDI moiety.

at the time position of the signal maximum. Both spectra exhibit the typical characteristics of light-induced triplet states[25] and can be unequivocally assigned to a single triplet species each. The spectral shape is entirely dominated by the zero-field splitting (ZFS) interaction arising from the dipolar coupling between the spins of both unpaired electrons[32]. The most important parameter in the Hamiltonian describing this interaction is the traceless ZFS tensor $\boldsymbol{D}$ characterised by the two parameters D and E. The former is proportional to r^{-3} with r being the distance between both unpaired electrons[32] and can therefore be related to the delocalisation length of the triplet exciton. The parameter E describes the rhombicity of the ZFS tensor. A vanishing E value leads to a axial system with D_x equal to D_y, whereas large E value give rise to a rhombic system. The ratio $\frac{E}{D}$ is hence a measure for the rhombicity and can not surpass the value of $\frac{1}{3}$ by definition. The rhombicity has

proven to be a sensitive probe for the molecular environment of the triplet exciton, including backbone planarity and aggregation effects[10,14,25,29,33]. Both parameters can be extracted from the experimental data by fitting spectral simulations. Comparing the spectra recorded for both potential repeat units with those previously reported for the polymer[11,14] reveal the similarity between the spectra of NDI-T2 and PNDIT2, hinting at a similar electronic structure, while the spectrum for T-NDI-T is clearly different from the spectra of both, NDI-T2 and polymer (cf. Fig. 3).

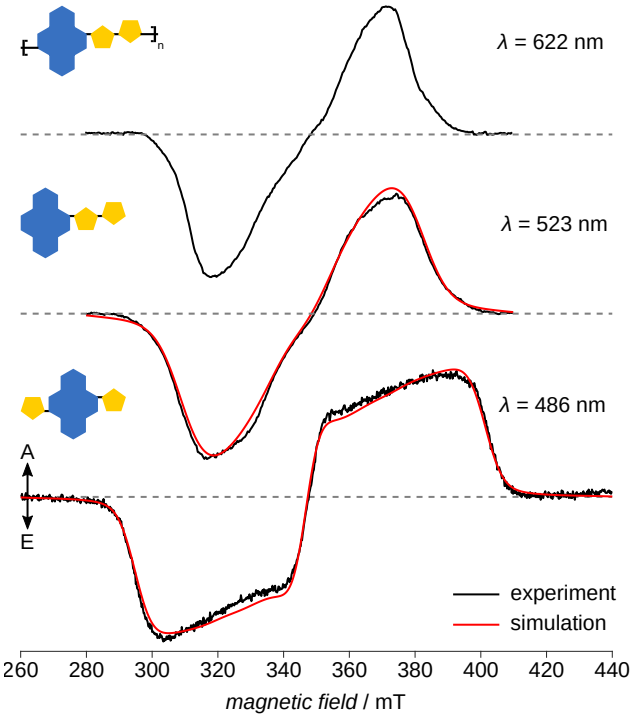

Figure 3: TREPR spectra of light-induced triplet states of T-NDI-T and NDI-T2 together with simulations (red lines) and the polymer PNDIT2. As TREPR spectroscopy uses a direct detection scheme, the spectra show emissive (E) and enhanced absorptive (A) signals directly. All samples were dissolved in 1-CN, flash-frozen and measured at 80 K with excitation at the maximum of their respective CT band. For simulation parameters, cf. Table 1 and for details of the fitting and simulations procedures, see the SI. Data for PNDIT2 were taken from Ref.[11].

For the spectra of both potential repeat units, simulations have been fitted to the experimental data. The simulation parameters are listed in Tab. 1, together with those for the polymer and other relevant building blocks. A larger D value is found for T-NDI-T, indicating a more localised triplet exciton compared to NDI-T2, in line with the results from optical spectroscopy (Fig. 2). Also a smaller rhombicity is found for the latter closer to that of the polymer, whereas T-NDI-T shows a fully rhombic spectrum. Large Gaussian line widths have been obtained for all simulations indicating the absence of aggregation in either of the compounds dissolved in 1-CN. Only one triplet sublevel of both potential repeat units is populated via inter-system crossing (ISC), p_2 for T-NDI-T and p_3 for NDI-T2, respectively, pointing towards different orbitals being involved in the ISC process. Comparing this to the situation in the polymer and the molecule T2-NDI-T2, respectively, provides further insight: While the triplet state populations of NDI-T2 and PNDIT2 are similar, with p_3 dominating, those of T-NDI-T resemble the situation in T2-NDI-T2, having the largest fraction on p_2. Taken together, both the rhombicity and the zero-field triplet sublevel populations of NDI-T2 are closer to the values obtained for the polymer than those of T-NDI-T.

To get further insight, density-functional theory (DFT) calculations of the singlet and triplet states and time-dependent DFT (TDDFT) calculations of the singlet ground state have been carried out for T-NDI-T, NDI-T2, as well as a polymer fragment. Different rotational conformers of the potential repeat units and the polymer fragment were geometry-optimised in their singlet ground state. For the polymer, a fragment of three monomers was used to represent the full molecule. Geometries and energy differences obtained for the singlet ground states are shown in Figs. S2 and S3. All geometries including the polymer fragment consist of flat NDI and thiophene moieties with substantial dihedral angles between adjacent units. Since further calculation of properties led to similar results for each conformer, only one conformer of each molecule was considered. The conformations chosen were those with the sulphur of the thiophenes pointing towards the

Table 1: Comparison of the simulation parameters of the triplet spectra of PNDIT2 and some of its fragments. The simulation parameters for the polymer PNDIT2 ($n = 13$) as well as the fragments NDI and T2-NDI-T2 are reproduced from Ref.[11]. The same trend already obvious from Fig. 3 can be seen in the simulation parameters: While the spectral shape and hence simulation parameters for NDI-T2 clearly resemble those of the polymer PNDIT2, the alternative building block T-NDI-T has a distinct electronic structure clearly different from the polymer. λ_{ex} (in nm) is the excitation wavelength used, corresponding to the maximum of the CT-band, D and E are the ZFS parameters (in MHz), Γ_L and Γ_G are the Lorentzian and Gaussian line widths (in mT) and $p_{1,2,3}$ are the populations of the triplet sublevels ordered from lowest to highest energy.

	λ_{ex}	$\lvert D\rvert$	$\lvert E\rvert$	$\lvert E\rvert/\lvert D\rvert$	Γ_G	Γ_L	$p_{1,2,3}$
T-NDI-T	486	1500 ± 0.8	500 ± 0.3	0.333	8.0 ± 0.3	3.0 ± 0.2	0.00, 1.00, 0.00
NDI-T2	523	1143 ± 2.0	308 ± 2.0	0.270	10.9 ± 0.6	6.5 ± 0.5	0.00, 0.00, 1.00
PNDIT2	622	1095 ± 4.3	226 ± 2.4	0.206	7.0 ± 0.8	2.1 ± 0.4	0.00, 0.24, 0.76
NDI	355	2073 ± 2.1	0	0.000	5.7 ± 0.3	2.8 ± 0.3	0.00, 0.50, 0.50
T2-NDI-T2	554	1010 ± 87.0	328 ± 84.9	0.325	11.4 ± 0.6	3.0 ± 0.6	0.00, 0.59, 0.41

oxygen of the NDIs, depicted in Fig. 4, consistent with the literature[11,24,34].

Single-point TDDFT[35] calculations allow to distinguish the orbitals involved in the electronic transition. The natural transition orbitals[36] (NTOs) of the holes and the particles for the first excited states are shown in Fig. 4, the corresponding excitation wavelengths are 524, 619 and 736 nm for T-NDI-T, NDI-T2 and the polymer fragment respectively. Compared with the experimentally obtained maxima of the CT band, all calculated excitations are redshifted by several tens of nanometres, but still in the range of the CT band. While this overestimation of the B3LYP functional is known[37], range-separated hybrid functionals like CAM-B3LYP[38] or ωB97X[39] did not yield better results. The holes, describing the NTO of the remaining non-excited electron, are mainly located on the donors. The particles, describing the NTO of the excited electron, are localised on the acceptors as expected for a CT transition[9,37,40]. Upon closer inspection of the holes, small delocalisations over the NDI units can be seen, most prominent for T-NDI-T. Also the thiophene to the left side of T-NDI-T is contributing more than the one on the right. For NDI-T2 and the polymer, the two linked thiophenes seem to act as one donor moiety, with a large contribution to the hole and only a very small contribution to the particle.

To investigate the triplet states of the molecules, the same conformers as for the singlet state were considered. These conformers were geometry-optimised in the triplet state accordingly and spin-density distributions calculated afterwards. For both potential repeat units and the polymer fragment, the Mulliken spin density of the triplet states of each atom, except the hydrogens, and the percentage of spin density on each unit is shown as a histogram in Fig. 5. T-NDI-T exhibits a fairly symmetrical distribution with respect to the axis connecting both nitrogen atoms of the NDI moiety. The triplet exciton is mostly localised on the NDI moiety with 72% and the amount of spin density on each single atom reflects the previously mentioned symmetrical distribution. NDI-T2 on the other hand exhibits a balanced distribution of spin density over both acceptor 48% and donor 52%, with a localisation around the NDI-thiophene bond. Similar to other investigated polymers[10,29], delocalisation of the triplet in the polymer is mostly restricted to one acceptor and the neighbouring donors, but otherwise pretty similar to that

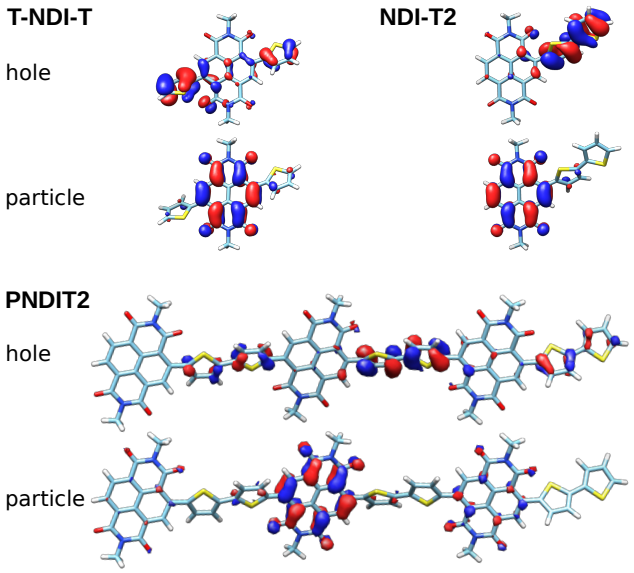

Figure 4: Natural transition orbitals (NTOs) of the hole-particle pairs of T-NDI-T, NDI-T2, and the polymer in their first excited singlet states. The B3LYP functional with the 6-31G** basis set was used. The corresponding eigenvalues λ denote the amount the two NTOs contribute to the transition. They are 0.9803 for T-NDI-T, 0.9892 for NDI-T2, and 0.9448 for the polymer. The NTOs are displayed for a threshold level of ± 0.03, red denotes a positive and blue a negative sign.

of NDI-T2. The main difference between the polymer and NDI-T2 is the additional spin density on the second T2 unit adjacent to the NDI moiety, but with one T2 unit clearly favoured. For both, NDI-T2 and polymer, the spin density remaining on the NDI stays nearly the same (only 4% difference), while the symmetrical spin-density distribution observed for T-NDI-T (and T2-NDI-T2[11]) vanishes entirely. Taken together, quantum-chemical calculations are consistent with the TREPR-spectroscopic investigations pointing towards a great similarity between NDI-T2 and PNDIT2 revealing a clearly asymmetric electronic structure, contrastring with T-NDI-T and T2-NDI-T2 being symmetrical.

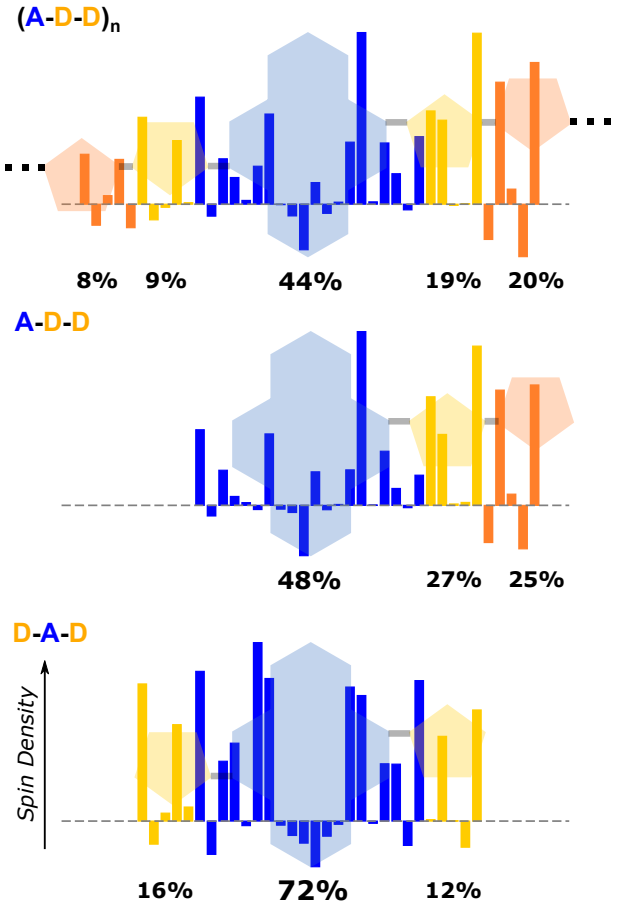

Figure 5: Mulliken spin density of both potential repeat units and the polymer. The atoms of the molecules have been labelled from left to right (for a detailed scheme, see Fig. S5). Geometries were optimised with the B3LYP functional and 6-31G** basis set. The numbers below the different units are the sum of the absolute values of the spin density localised on each of the moieties.

Discussion

Optical spectroscopy reveals differences in the delocalisation of the exciton of T-NDI-T and NDI-T2 that are consistent with the triplet exciton delocalisation probed by TREPR spectroscopy, but it is inconclusive with respect to revealing details of the electronic structure and its similarity to that of the polymer. TREPR spectroscopy, in contrast, provides the necessary molecular resolution and unequivocally reveals NDI-T2 to be the actual repeat unit of PNDIT2 in terms of its electronic structure, as obvious from comparing the TREPR spectra of

T-NDI-T, NDI-T2, and the polymer PNDIT2 (Fig. 3). The simulation parameters reported in Tab. 1 confirm this result. The rhombicity and also the zero-field triplet sublevel populations of NDI-T2 are closer to those of the polymer than those of T-NDI-T. DFT calculations of the spin density lead to the same conclusion. The only 48 MHz smaller D value (approx. 5%) for the polymer, compared to NDI-T2, indicates that the triplet exciton is only slightly more delocalised. The same is reflected in the spin density distribution of the polymer, where 83% remain on the NDI-T2 fragment and 17% on the other neighbouring T2.

T-NDI-T shows a larger D value than NDI-T2 indicating a more localised triplet exciton, consistent with the strong localisation of 72% the spin density on the NDI moiety predicted by DFT calculations. Both results hint at NDI and T-NDI-T having a similar electronic structure. Comparing their TREPR spectra[11] reveals, however, clear differences: While NDI shows a larger D value than T-NDI-T, to be expected due to the smaller size, its spectrum is fully axial in stark contrast to the fully rhombic one of T-NDI-T. Also the zero-field triplet sublevel populations are different with p_2 and p_3 being populated equally for NDI, whereas only p_2 is populated for T-NDI-T (Tab. 1), pointing towards different orbitals involved in the ISC transition. NDI and T-NDI-T hence clearly show a markedly different electronic structure. A second molecule T-NDI-T should be compared to is the larger D-A-D system T2-NDI-T2[11]. The TREPR spectrum of the latter resembles that of T-NDI-T, particularly when comparing the rhombicity and triplet sublevel populations, leading to the same conclusion: the two building blocks considered here, T-NDI-T and NDI-T2, strongly differ from each other with respect to their electronic structures. This provides interesting hints for understanding the markedly different electronic structure of T2-NDI-T2 compared to PNDIT2 and all other fragments investigated previously:[11] The electronic structure of PNDIT2 is dominated by an intrinsically asymmetric chromophore, NDI-T2, with a single T2 unit predominantly acting as donor for one NDI acceptor unit.

Furthermore, the results of quantum-chemical calculations provide confirmation for the differences in exciton delocalisation between NDI-T2 and T-NDI-T. Delocalisation seems to be connected to the strength of the donor–acceptor interaction and hence CT character: the larger the CT character, the larger the delocalisation, as revealed by comparing the NTOs (Fig. 4). Additionally, the more localised singlet exciton on the acceptor moiety for T-NDI-T could explain the better resolved vibrational structure of the NDI unit in this molecule. Similarly, the localised spin density of the triplet exciton of T-NDI-T represents a weak donor–acceptor interaction and the broad homogeneous distribution of NDI-T2 a strong one. This is in line with previous investigations of PCDTBT, another push–pull copolymer, with a strong localisation of the spin density on the dominant acceptor and donor units of the molecule[10]. Taken together, these results show a strong donor–acceptor interaction to be characterised by a homogeneous spin density distribution on donor and acceptor moieties. Furthermore, the consistency between optical and TREPR results proves the validity and relevance of the results obtained by investigating the triplet states for the overall electronic structure of the molecule and demonstrates TREPR spectroscopy to be superior to optical spectroscopy in this respect.

Conclusions

Knowing the repeat unit of a conjugated push-pull copolymer is essential for a detailed understanding of the structure–function relationship of, but not resticted to, conjugated polymers used in organic electronics applications. Hence, spectroscopic tools providing the necessary molecular resolution that allows to discriminate between different building blocks and to decide which one actually resembles the electronic structure of the polymer are of utmost importance. Here, we demonstrate TREPR spectroscopy to be perfectly suited for this task, due to its molecular resolution and unique capability of using light-induced triplet states to probe the electronic structure as well as the impact of

the local environment, and to be clearly superior to steady-state optical spectroscopy. Once the actual repeat unit in terms of its electronic structure has been identified, it can serve as a model for the entire copolymer with alternating donor and acceptor moieties.[10,11,29] Our results for the polymer PNDIT2 and the two possible repeat units T-NDI-T and NDI-T2 reveal NDI-T2 unambiguously as the "true" repeat unit of the polymer in terms of its electronic structure. This is essential for getting insight into the structure–function relationship of the polymer. Furthermore, TREPR spectroscopy and accompanying quantum-chemical calculations reveal the asymmetry of the NDI-T2 moiety to dominate the electronic structure of the polymer, providing guidelines for the rational design of new and improved materials.

Materials and Methods

Synthesis

NDI-T2 and T-NDI-T were synthesised according to published procedures[41,42].

UV-VIS spectroscopy

NDI-T2 and T-NDI-T were dissolved in 1-chloronaphthalene (1-CN) with a concentration $c = 1.3$ mg/mL (NDI-T2) and $c = 1.0$ mg/mL (T-NDI-T), respectively. UV-VIS experiments were performed with commercially available spectrometers at room temperature. For details of the experimental setup see the SI.

TREPR spectroscopy

Samples were prepared identically to those of the optical experiments in terms of concentrations and filled into synthetic-quartz-glass tubes. TREPR experiments were carried out on frozen solutions at cryogenic temperatures (80 K). For better comparison with the previous experiments[11], samples were flash-frozen in liquid nitrogen to preserve the morphology in solution. Each sample was excited at the maximum of its charge transfer (CT) band with a pulse energy of 1 mJ, using an optical parametric oscillator (OPO) pumped by a Nd:YAG laser. The laser light was depolarised in order to prevent polarisation effects as PNDIT2 and its building blocks have been shown to be sensitive to remaining polarisation of the laser light used for excitation[43]. Spectral simulations have been fitted to the experimental data using the Tsim program[44] which builds upon the `pepper` routine of the EasySpin toolbox[45]. Further details of the experimental setup and parameters are given in the SI.

DFT calculations

All initial molecular geometries were created with Avogadro 1.2.0[46]. DFT calculations were carried out using the ORCA program package[47]. In a first step, the geometries of the singlet ground state and the triplet state were optimised using the B3LYP functional[48,49], 6-31G** basis set[50,51] and D3 dispersion correction[52]. Afterwards, linear response TDDFT calculations were performed on the optimised singlet geometries using the Tamm-Dancoff approximation[53] in conjunction with B3LYP/6-31G** as functional and basis set, respectively. The Coulomb term was handled with the resolution of identity chain of spheres approximation (RIJCOSX)[54] to increase calculation speed. Geometries and spin density delocalisations of the triplet states of all considered rotamers are shown in Figs. S2–4. All figures showing molecular geometries and spin densities were created using UCSF Chimera 1.11.2.[55]

Acknowledgement The authors thank the German Research Foundation (DFG, Grants GRK 1642 to C.M., R.M., and M.So., SO 1213/8-1 to R.M. and M.So., and BI 1249/3-1 to T.B.) for financial support, and S. Weber and C. Kay for providing EPR equipment.

Supporting Information Available

Details of experiments, simulations and the fitting procedure; different conformers in singlet

ground state; spin-density distribution for the triplet states; atom labelling scheme for Fig. 5.

Author information

Corresponding author: Till Biskup, research@till-biskup.de

The authors declare no competing financial interest.

References

(1) Chiang, C. K.; Fincher, C. R., Jr.; Park, Y. W.; Heeger, A. J.; Shirakawa, H.; Louis, E. J.; Gau, S. C.; MacDiarmid, A. G. Electrical conductivity in doped polyacetylene. *Phys. Rev. Lett.* **1977**, *39*, 1098–1101.

(2) Shirakawa, H.; Louis, E. J.; MacDiarmid, A. G.; Chiang, C. K.; Heeger, A. J. Synthesis of electrically conducting organic polymers: halogen derivatives of polyacetylene, $(CH)_x$. *J. Chem. Soc. Chem. Commun.* **1977**, *1977*, 678–580.

(3) Heeger, A. J. Semiconducting and metallic polymers: the fourth generation of polymeric materials (Nobel lecture). *Angew. Chem. Int. Ed.* **2001**, *40*, 2591–2611.

(4) Cheng, Y.-J.; Yang, S.-H.; Hsu, C.-S. Synthesis of conjugated polymers for organic solar cell applications. *Chem. Rev.* **2009**, *109*, 5868–5923.

(5) Facchetti, A. Polymer donor–polymer acceptor (all-polymer) solar cells. *Mater. Today* **2013**, *16*, 123–132.

(6) Armin, A.; Li, W.; Sandberg, O. J.; Xiao, Z.; Ding, L.; Nelson, J.; Neher, D.; Vandewal, K.; Shoaee, S.; Wang, T. et al. A history and perspective of non-fullerene electron acceptors for organic solar cells. *Adv. Energy Mater.* **2021**, *11*, 20003570.

(7) Schwoerer, M.; Wolf, H. C. *Organische Molekulare Festkörper*; WILEY-VCH: Weinheim, Germany, 2005.

(8) Köhler, A.; Bässler, H. *Electronic Processes in Organic Semiconductors*; WILEY-VCH: Weinheim, Germany, 2015.

(9) Banerji, N.; Gagnon, E.; Morgantini, P.-Y.; Valouch, S.; Mohebbi, A. R.; Seo, J.-H.; Leclerc, M.; Heeger, A. J. Breaking down the problem: optical transitions, electronic structure, and photoconductivity in conjugated polymer PCDTBT and in its separate building blocks. *J. Phys. Chem. C* **2012**, *116*, 11456–11469.

(10) Matt, C.; Meyer, D. L.; Lombeck, F.; Sommer, M.; Biskup, T. TBT entirely dominates the electronic structure of the conjugated copolymer PCDTBT: Insights from time-resolved electron paramagnetic resonance spectroscopy. *Macromolecules* **2018**, *51*, 4341–4349.

(11) Meyer, D. L.; Matsidik, R.; Sommer, M.; Biskup, T. Electronic structure trumps planarity: Unexpected narrow exciton delocalisation in PNDIT2 revealed by time-resolved EPR spectroscopy. *Adv. Electron. Mater.* **2018**, *4*, 1700384.

(12) Mavrommati, S. A.; Skourtis, S. S. Initial-state preparation effects in time- resolved electron paramagnetic resonance experiments. *J. Chem. Phys.* **2020**, *152*, 044304.

(13) Meyer, D. L.; Schmidt-Meinzer, N.; Matt, C.; Rein, S.; Lombeck, F.; Sommer, M.; Biskup, T. Side-chain engineering of conjugated polymers: Distinguishing its impact on film morphology and electronic structure. *J. Phys. Chem. C* **2019**, *123*, 20071–20083.

(14) Meyer, D. L.; Matsidik, R.; Huettner, S.; Sommer, M.; Biskup, T. Solvent-mediated aggregate formation of PNDIT2: Decreasing the available conformational subspace by introducing locally highly ordered domains. *Phys. Chem. Chem. Phys.* **2018**, *20*, 2716–2723.

(15) Meyer, D. L.; Matsidik, R.; Fazzi, D.; Sommer, M.; Biskup, T. Probing exciton

delocalization in organic semiconductors: Insight from time-resolved electron paramagnetic resonance and magnetophotoselection experiments. *J. Phys. Chem. Letters* **2018**, *9*, 7026–7031.

(16) Zhou, N.; Facchetti, A. Naphthalenediimide (NDI) polymers for all-polymer photovoltaics. *Mater. Today* **2018**, *21*, 377–390.

(17) Earmme, T.; Hwang, Y.-J.; Murari, N. M.; Subramaniyan, S.; Jenekhe, S. A. All-polymer solar cells with 3.3% efficiency based on naphthalene diimide-selenophene copolymer acceptor. *J. Am. Chem. Soc.* **2013**, *135*, 14960–14963.

(18) Sharma, S.; Kolhe, N. B.; Gupta, V.; Bharti, V.; Sharma, A.; Datt, R.; Chand, S.; Asha, S. K. Improved all-polymer solar cell performance of n-type naphthalene diimide–bithiophene P(NDI2OD-T2) copolymer by incorporation of perylene diimide as coacceptor. *Macromolecules* **2016**, *49*, 8113–8125.

(19) Schmidt, S. B.; Hönig, M.; Shin, Y.; Cassinelli, M.; Perinot, A.; Caironi, M.; Jiao, X.; McNeill, C. R.; Fazzi, D.; Biskup, T. et al. Radical anion yield, stability, and electrical conductivity of naphthalene diimide copolymers n-doped with tertiary amines. *ACS Appl. Polym. Mater.* **2020**, *2*, 1954–1963.

(20) Steyrleuthner, R.; Schubert, M.; Howard, I.; Klaumünzer, B.; Schilling, K.; Chen, Z.; Saalfrank, P.; Laquai, F.; Facchetti, A.; Neher, D. Aggregation in a high-mobility n-type low-bandgap copolymer with implications on semicrystalline morphology. *J. Am. Chem. Soc.* **2012**, *134*, 18303–18317.

(21) Brinkmann, M.; Gonthier, E.; Bogen, S.; Tremel, K.; Ludwigs, S.; Hufnagel, M.; Sommer, M. Segregated *versus* mixed interchain stacking in highly oriented films of naphthalene diimide bithiophene copolymers. *ACS Nano* **2012**, *6*, 10319–10326.

(22) Tremel, K.; Fischer, F. S. U.; Kayunkid, N.; Di Pietro, R.; Tkachov, R.; Kiriy, A.; Neher, D.; Ludwigs, S.; Brinkmann, M. Charge transport anisotropy in highly oriented thin films of the acceptor polymer P(NDI2OD-T2). *Adv. Energy Mater.* **2014**, *4*, 1301659.

(23) Giussani, E.; Brambilla, L.; Fazzi, D.; Sommer, M.; Kayunkid, N.; Brinkmann, M.; Castiglioni, C. Structural characterization of highly oriented naphthalene-diimide-bithiophene copolymer films via vibrational spectroscopy. *J. Phys. Chem. B* **2015**, *119*, 2062–2073.

(24) Caironi, M.; Bird, M.; Fazzi, D.; Chen, Z.; Di Pietro, R.; Newman, C.; Facchetti, A.; Sirringhaus, H. Very low degree of energetic disorder as the origin of high mobility in an *n*-channel polymer semiconductor. *Adv. Funct. Mater.* **2011**, *21*, 3371–3381.

(25) Biskup, T. Structure–function relationship of organic semiconductors: Detailed insights from time-resolved EPR spectroscopy. *Front. Chem.* **2019**, *7*, 10.

(26) Weber, S. Transient EPR. *eMagRes* **2017**, *6*, 255–270.

(27) Forbes, M. D.; Jarocha, L. E.; Sim, S.; Tarasov, V. F. Time-resolved electron paramagnetic resonance spectroscopy: history, technique, and application to supramolecular and macromolecular chemistry. *Adv. Phys. Org. Chem.* **2014**, *47*, 1–83.

(28) Biskup, T.; Sommer, M.; Rein, S.; Meyer, D. L.; Kohlstädt, M.; Würfel, U.; Weber, S. Ordering of PCDTBT revealed by time-resolved electron paramagnetic resonance spectroscopy of its triplet excitons. *Angew. Chem. Int. Ed.* **2015**, *54*, 7707–7710.

(29) Matt, C.; Lombeck, F.; Sommer, M.; Biskup, T. Impact of side chains of conjugated polymers on electronic structure: A case study. *Polymers* **2019**, *11*, 870.

(30) Alp, S.; Şule Erten,; Karapire, C.; Köz, B.; Doroshenko, A. O.; Içli, S. Photoinduced energy–electron transfer studies with naphthalene diimides. *J. Photochem. Photobiol. A Chem.* **2000**, *135*, 103–110.

(31) Hintze, C.; Steiner, U. E.; Drescher, M. Photoexcited triplet state kinetics studied by electron paramagnetic resonance spectroscopy. *ChemPhysChem* **2017**, *18*, 6–16.

(32) Atherton, N. M. *Principles of Electron Spin Resonance*; Ellis Horwood Ltd.: Chichester, England, 1993.

(33) Matt, C.; Stry, K.; Matsidik, R.; Sommer, M.; Biskup, T. Two competing acceptors: Electronic structure of PNDITBT probed by time-resolved electron paramagnetic resonance spectroscopy. *J. Chem. Phys.* **2019**, *151*, 234901.

(34) Fazzi, D.; Caironi, M. Multi-length-scale relationships between the polymer molecular structure. *Phys. Chem. Chem. Phys.* **2015**, *17*, 8573–8590.

(35) Runge, E.; Gross, E. K. U. Density-functional theory for time-dependent systems. *Phys. Rev. Lett.* **1984**, *52*, 997–1000.

(36) Martin, R. L. Natural transition orbitals. *J. Chem. Phys.* **2003**, *118*, 4775.

(37) Pan, Y. Y.; Huanga, J.; Wanga, Z. M.; Zhangb, S. T.; Yua, D. W.; Yang, B.; Mac, Y. G. Accurate description of hybridized local and charge-transfer excited-state in donor–acceptor molecules using density functional theory. *RSC Adv.* **2016**, *6*, 108404–108410.

(38) Yanai, T.; Tew, D. P.; Handy, N. C. A new hybrid exchange–correlation functional using the Coulomb-attenuating method (CAM-B3LYP). *Chem. Phys. Lett.* **2004**, *393*, 51–57.

(39) Chai, J.-D.; Head-Gordon, M. Systematic optimization of long-range corrected hybrid density functionals. *J. Chem. Phys.* **2008**, *128*, 084106.

(40) Zhou, C.; Xiao, S.; Wang, M.; Jiang, W.; Liu, H.; Zhang, S.; Yang, B. Modulation of excited state property based on benzo[a, c]phenazine acceptor: three typical excited states and electroluminescence performance. *Front. Chem.* **2019**, *7*, 141.

(41) Matsidik, R.; Komber, H.; Luzio, A.; Caironi, M.; Sommer, M. Defect-free naphthalene diimide bithiophene copolymers with controlled molar mass and high performance via direct arylation polycondensation. *J. Am. Chem. Soc.* **2015**, *137*, 6705–6711.

(42) Matsidik, R.; Martin, J.; Schmidt, S.; Obermayer, J.; Lombeck, F.; Nübling, F.; Komber, H.; Fazzi, D.; Sommer, M. C–H arylation of unsubstituted furan and thiophene with acceptor bromides: Access to donor–acceptor–donor-type building blocks for organic electronics. *J. Org. Chem.* **2015**, *50*, 980–987.

(43) Meyer, D. ESR-spektroskopische Untersuchungen lichtinduzierter Zustände in Materialien mit Relevanz für die organische Elektronik. Morphologie, Delokalisation, Entstehungswege von Triplett-Zuständen. Ph.D. thesis, Albert-Ludwigs-Universität Freiburg, 2017.

(44) Meyer, D. L.; Lombeck, F.; Huettner, S.; Sommer, M.; Biskup, T. Direct $S_0 \rightarrow T$ excitation of a conjugated polymer repeat unit: unusual spin-forbidden transitions probed by time-resolved electron paramagnetic resonance spectroscopy. *J. Phys. Chem. Letters* **2017**, *8*, 1677–1682.

(45) Stoll, S.; Schweiger, A. EasySpin, a comprehensive software package for spectral simulation and analysis in EPR. *J. Magn. Reson.* **2006**, *178*, 42–55.

(46) Hanwell, M. D.; Curtis, D. E.; Lonie, D. C.; Vandermeersch, T.; Zurek, E.; Hutchison, G. R. Avogadro: an advanced semantic chemical editor, visualization, and analysis platform. *J. Cheminformatics* **2012**, *4*, 17.

(47) Neese, F. The ORCA program package. *Wiley Interdiscip. Rev.-Comput. Mol. Sci.* **2012**, *2*, 73–78.

(48) Becke, A. D. Density-functional thermochemistry. III. The role of exact exchange. *J. Chem. Phys.* **1993**, *98*, 5648–5652.

(49) Lee, C.; Yang, W.; Parr, R. G. Development of the Colle-Salvetti correlation-energy formula into a functional of the electron density. *Phys. Rev. B* **1988**, *37*, 785–789.

(50) Petersson, G. A.; Bennett, A.; Tensfeldt, T. G.; Al-Laham, M. A.; Shirley, W. A.; Mantzaris, J. A complete basis set model chemistry. I. The total energies of closed-shell atoms and hydrides of the first-row elements. *J. Chem. Phys.* **1988**, *89*, 2193–2218.

(51) Petersson, G. A.; Al-Laham, M. A. A complete basis set model chemistry. II. Open-shell systems and the total energies of the first-row atoms. *J. Chem. Phys.* **1991**, *94*, 6081–6090.

(52) Grimme, S.; Antony, J.; Ehrlich, S.; Krieg, H. A consistent and accurate ab initioparametrization of density functionaldispersion correction (DFT-D) for the 94 elements H–Pu. *J. Chem. Phys.* **2010**, *132*, 154104.

(53) Grimme, S. A simplified Tamm-Dancoff density functional approach for the electronic excitation spectra of very large molecules. *J. Chem. Phys.* **2013**, *138*, 244104.

(54) Neese, F.; Wennmohs, F.; Hansen, A.; Becker, U. Efficient, approximate and parallel Hartree–Fock and hybrid DFT calculations. A 'chain-of-spheres' algorithm for the Hartree–Fock exchange. *Chem. Phys.* **2009**, *356*, 98–109.

(55) Pettersen, E. F.; Goddard, T. D.; Huang, C. C.; Couch, G. S.; Greenblatt, D. M.; Meng, E. C.; Ferrin, T. E. UCSF Chimera—A visualization system for exploratory research and analysis. *J. Comput. Chem.* **2004**, *25*, 1605–1612.